UNITED NATIONS UNIVERSITY
GEOTHERMAL TRAINING PROGRAMME
Orkustofnun, Grensásvegur 9,
IS-108 Reykjavík, Iceland

Reports 2008
Number 14

COMPARATIVE STUDY ON THE HIGH-TEMPERATURE FIELDS OF HVERAVELLIR IN ICELAND AND TENDAHO IN ETHIOPIA

Gezahegn Daba
Geological Survey of Ethiopia
Hydrogeology, Engineering Geology and Geothermal Department
P.O. Box 2302, Addis Ababa
ETHIOPIA
geda_nig@yahoo.com

ABSTRACT

Geochemistry plays an important role in geothermal science from the exploration phase up to monitoring of fluids after a power plant has been established. In this report, several geochemical methods have been applied to evaluate reservoir temperature and processes happening in the upflow zones of the two high-temperature fields in Iceland and Ethiopia. Hveravellir is one of the high-temperature geothermal areas of Iceland. Binary plots of Cl vs. cations, B and TDS and Na-K-Mg ternary plot show that the water from this field has undergone boiling and mixing in the upflow zone. The water from the hot springs of Hveravellir is rich in silica, up to 662 mg/l. The various types of silica geothermometers gave temperature results ranging between 197 and 319°C. Tendaho high-temperature geothermal field is one of two potential geothermal areas in the Ethiopian rift where drilling has been done and found to be productive, the other being the Aluto-Langano field. Similar geochemical methods have been applied to this geothermal field as at Hveravellir. The methods used show that the field has undergone mixing with cold water in the upflow zone. The reservoir temperature of the area, according to different types of silica geothermometers, is in the range 210-280°C, while various types of Na-K geothermometers gave the temperature results of 167-225°C. The discrepancy may be due to cold water mixing.

1. INTRODUCTION

The objective of this study is to compare geochemical results from the two high-temperature areas Hveravellir in Iceland and Tendaho in Ethiopia through geochemical evaluation of the conditions of mineral equilibria and the estimation of sub surface temperatures from geothermal fluids of the wells and hot springs. This study also assesses mixing processes that affect the compositions of the geothermal fluids in the upflow zone before reaching the springs and wells. Hydrogeological characteristics of the area will also be assessed.

Iceland is located on the Mid-Atlantic Ridge at the diverging plate boundaries of the American and European plates. The spreading direction is N100°E and the drift velocity is about 1cm/year (Björnsson, 1985). The volcanic rift zone crosses Iceland from southwest to northeast. It is the land

ward continuation of the axial area of the Mid-Atlantic Ridge. It is characterized by active volcanoes, fissure swarms, numerous normal faults and high-temperature geothermal fields. Over 23 high-temperature fields are known in Iceland. The Hveravellir field is one of them (Figure 1).

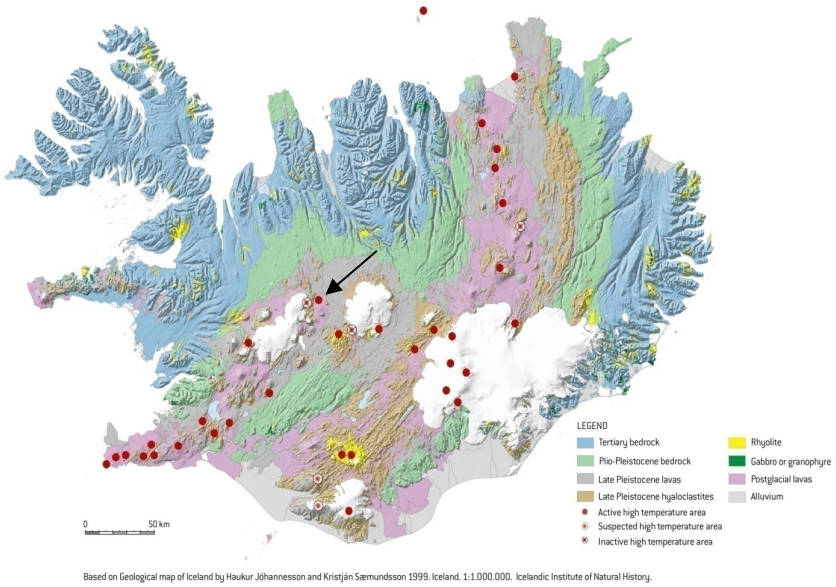

FIGURE: 1: Geological and high-temperature geothermal map of Iceland, the arrow points at the Hveravellir geothermal field

The Ethiopian rift is a part of the larger Great East African Rift Valley. It is a continental rift zone that appears to be a developing divergent tectonic plate boundary. The rift is a narrow zone in which the African plate is in the process of splitting into two new plates called the Nubian and Somalian sub plates or protoplates. It runs from the Afar triple junction in the Afar depression southward through east Africa. The Afar triangle is an area of active extensional tectonics and basaltic magmatism from which the Gulf of Aden, the Red Sea and the Ethiopian Rift System radiate.

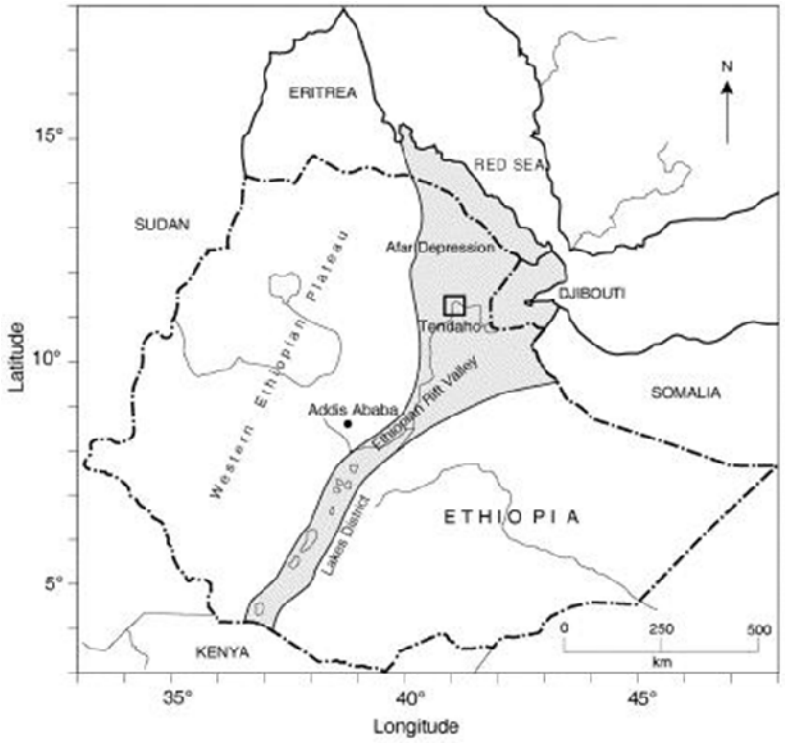

FIGURE 2: The Ethiopian Rift System and the location of the Tendaho high-tempeature field

The Tendaho geothermal field is located at the junction of the Northern Afar and the southern Afar rift valleys (Figure 2). This geothermal field is one of several geothermal fields in the Ethiopian rift valley which was identified as a high-temperature area during the early reconnaissance survey that started in 1969 (UNDP, 1973). After detailed geological, geophysical and geochemical studies, six exploration wells were drilled in the area. Three of the wells are deep, reaching to 2000 m. One deep well and three shallow wells are productive. In this study, samples from one of the production wells, TD-6, are analysed.

Several classification schemes have been proposed for geothermal systems in the world. The tradition in Iceland and Ethiopia is to divide them into two groups, high- and low-temperature fields. This division has also proved to be practical elsewhere around the globe. The main characteristics of the two groups are given in Table 1.

TABLE 1: A classification of geothermal systems

Low-temperature field	High-temperature field
Outside the volcanic zone	Inside the volcanic zone
Temperatures less than 150°C at 1 km depth	Temperature 200-300°C at 1-3 km depth
Heat source: High heat flow and convective heat mining	Heat source: Cooling magma bodies
Usually low in chemical content	Usually high in chemical content
Suitable for direct uses such as space heating, heat pumps, balneology, fish farming, snow melting, etc.	Suitable for electricity production, indirect space heating, etc.

2. SAMPLING AND ANALYTICAL METHODS

Sampling of geothermal fluids presents some problems not encountered when sampling surface and cold groundwaters. Specific collection techniques are required to obtain representative samples because of the elevated temperature and boiling of these fluids, the effect of exposing them to the atmosphere and cooling of the samples.

A total of 9 samples for Hveravellir and 13 samples for Tendaho were collected for chemical analysis, out of which one is cold water from Hveravellir. The standard procedures as outlined by Giggenbach and Goguel (1989) and Fahlquist and Janic (1992) were used for sample collection. Water samples were collected in 125, 250 and 500 ml polyethylene bottles. Samples for cations determinations were acidified with HNO_3. Before acidifying samples for cation analysis, the samples were filtered with a 0.45 μm pore size acetate membrane. All the bottles were rinsed three times with the sampled water. Samples for measuring silica were diluted 1:10 with distilled water and samples for measuring H_2S are treated with ZnAc for precipitating sulphide which otherwise could interfere with sulphate measurements. Outlet temperature and pH were determined directly in the field. Chemical analysis for the water from Hveravellir and Tendaho were performed at the ISOR and Ethiopian central geological laboratories by the methods summarized in Table 2.

TABLE 2: Analytical methods for geothermal fluids

Component	Sample treatment	Methods of analysis
CO_2	Ru	Alkalinity-titration
H_2S	Ru	Titration
SiO_2	Rd	Spectrophotometry
Na, K, Ca, Al, Fe	Fa	Atomic absorption spectrometry
Cl, F	Ru	Ion chromatography
SO_4	Fp	Ion chromatography
$\delta^{18}O$,δD	Ru	Mass spectrometry
PH	Ru	Ion Selective electrode

Ru: Raw and untreated; Rd: Raw and diluted;
Fp: Filtered and precipitated; Fa: Filtered and acidified

3. GEOCHEMICAL METHODS IN GEOTHERMAL EXPLORATION

Geochemistry plays an important role during geothermal exploration drillings and later development of geothermal reservoirs. Here, geochemistry provides data on the chemical properties of the discharged fluid, the level and temperature of producing aquifers in the wells and steam to water ratios

in the reservoir. In this way, geochemistry contributes to the overall understanding of the production characteristics of the geothermal reservoir; it also quantifies scaling and corrosion tendencies. After utilisation has been initiated, geochemical monitoring is one of the most useful tools in mapping the response of the reservoir to the production load, including recharge, pressure drawdown and enhanced boiling.

Geochemical methods are relatively inexpensive and can provide valuable information on the temperature conditions in the geothermal reservoir and the source of the geothermal fluid. The use of geochemistry in geothermal exploration has a profound importance in inferring subsurface conditions by studying the chemistry of surface manifestations or discharge fluids that carry the signature of the geothermal system.

The chemical composition in a fluid moving through fractures and porous spaces will be modified spatially and temporally, by chemical interactions with the bedrock and/or by mixing with other fluids. The chemical composition of the parent fluid is either conserved, keeping the original composition, or modified through the flow paths controlled by the flow media. Chemically inert constituents that are conserved and not changed by chemical reactions provide information on the sources of the fluid. Such sources are termed tracers. On the other hand, reactive components, such as SiO_2, CO_2, H_2S etc., react with the minerals and other reactive constituents and can contain information about the subsurface conditions. Such components are called geoindicators (Arnórsson, 2000). Geothermometers are geoindicators that can be used to estimate subsurface temperature using the chemical and isotopic compositions of discharges.

3.1 Geothermometry

Chemical and isotope geothermometers probably constitute the most important geochemical tool for the exploration and development of geothermal resources. They are also very important during exploitation in monitoring the response of geothermal reservoirs to the production load. Geothermometers have been classified into three groups (D'Amore and Arnórsson, 2000):

1. Water and solute geothermometers;
2. Steam and gas geothermometers;
3. Isotope geothermometers.

The most widely used geothermometers are based on silica concentrations, cation ratios (mainly Na/K), and gas ratios and concentrations in the steam phase. Selected geothermometers of these types are described below.

3.1.1 Silica geothermometers

The increased solubility of quartz and its polymorphs at elevated temperature has been used extensively as an indicator of geothermal temperatures (Truesdell and Hulston, 1980; Fournier and Potter, 1982). In systems above 180-190°C, equilibrium with quartz has been found to control the silica concentration, whereas at lower temperatures, chalcedony is the controlling phase (Árnason, 1976). When plotting the logarithm of dissolved silica versus the inverse of the absolute temperature, the data for several silica minerals (quartz, chalcedony, α-cristobalite, opal-CT, and amorphous silica) lie along straight lines in the 20-250°C range, even in the residual water after single-step steam separation at 100°C (Morey et al., 1962; Fournier and Rowe, 1962). Generally speaking, the quartz geothermometer is applied in high-temperature reservoirs, and the chalcedony geothermometer in low-temperature reservoirs.

Temperature can be derived from the following relationships for equilibrium with these silica polymorphs from 0 to 250°C, where Si concentrations are in ppm (from Fournier, 1981):

Quartz (no steam loss):
$$T\ (°C) = \frac{1309}{5.19 - \log s} - 273.5 \quad (1)$$

Quartz (maximum steam loss):
$$T\ (°C) = \frac{1522}{5.75 - \log s} - 273.5 \quad (2)$$

Chalcedony:
$$T\ (°C) = \frac{1032}{4.69 - \log s} - 273.5 \quad (3)$$

Amorphous silica:
$$T\ (°C) = \frac{731}{4.52 - \log s} - 273.5 \quad (4)$$

3.1.2 Cation geothermometers

Studies of Na, K and Ca in aqueous systems suggest that cation concentrations are controlled by temperature dependent equilibrium reactions with feldspars, mica and calcite. Of the cation geothermometers, the Na-K geothermometer is the most widely used geothermometer. The Na-K ratio was initially used to identify the upflow zone of a geothermal system, where the lowest values are observed at the centre of the upflow zone (Ellis and Wilson, 1960). Since then, this method has evolved to increasingly more precise calibration of the temperature dependence of the Na/K ratio, resulting in the calibration of the Na/K geothermometer.

The Na-K geothermometer generally gives consistent results for near neutral pH of geothermal waters that have low calcium content, ($\sqrt{Ca}/\sqrt{Na}$) <1. The Na/K geothermometers are generally in agreement with quartz geothermometers but sometimes they yield rather high results (Ellis and Mahon, 1977). A general decrease in Na/K ratios of thermal waters with increasing temperatures was observed long ago (Ellis and Wilson, 1960). The initial attempts to derive, from these observations, on empirical Na-K geothermometer led to equations (White, 1965, Ellis and Mahon, 1977) with relatively small temperature dependencies, due to the inclusion in the data sets of poorly equilibrated spring waters.
A calibration equation with high-temperature dependence was proposed by Fournier and Truesdell (1973). They took into account experimental data on cation exchanges between coexisting Na-and K-feldspars (Orville, 1963). The relationships proposed later by Truesdell (1975) and Arnórsson et al. (1983) did not lead to substantial modifications. A step forward was done by Fournier (1979), who carried out an empirical calibration based on well equilibrated water discharges from deep geothermal wells and oil field brines. In fact, the equation proposed by Fournier (1979):

$$T\ (°C) = \frac{1217}{1.483 - \log(Na/K)} - 273.5 \quad (5)$$

closely approaches that computed by means of thermodynamic data of Na-and K-feldspars.

Another empirical relationship, characterized by slightly steeper temperature dependencies, was suggested by Giggenbach et al. (1983) and Giggenbach (1988):

$$T\ (°C) = \frac{1390}{1.75 - \log(Na/K)} - 273.5 \quad (6)$$

The cation geothermometers considered in this study are listed below; Na and K refer to the concentrations of these cations in ppm:

$$T\ (°C) = \frac{856}{0.857 - \log(Na/K)} - 273.5 \quad (7)$$

$$T\ (°C) = \frac{883}{0.78 - \log(^{Na}/_{K})} - 273.5 \quad (8)$$

$$T\ (°C) = \frac{933}{0.993 - \log(^{Na}/_{K})} - 273.5 \quad (9)$$

$$T\ (°C) = \frac{1319}{1.699 - \log {}^{Na}/_{K}} - 273.5 \quad (10)$$

$$T\ (°C) = \frac{1217}{1.483 - \log(^{Na}/_{K})} - 273.5 \quad (11)$$

$$T\ (°C) = \frac{1178}{1.47 - \log(^{Na}/_{K})} - 273.5 \quad (12)$$

$$T\ (°C) = \frac{1390}{1.75 - \log(^{Na}/_{K})} - 273.5 \quad (13)$$

Equation 7 is from Truesdell and Fournier (1976), Equation 8 from Tonani (1980) and Equations 9 and 10 are from Arnórsson et al. (1983). Equation 11 is from Fournier, (1979), and Equation 12 from Nieva and Nieva (1987), while Equation 13 is from Giggenbach et al. (1983).

3.2 The Cl-SO_4-HCO_3 triangular plot

The Cl-SO_4-HCO_3 triangular plot is used for an initial classification of geothermal water samples (Giggenbach, 1988; Giggenbach and Goguel, 1989). The position of a data point in this plot is obtained by first calculating the sum Σ of the concentrations C (mg/kg) of all the species involved:

$$\Sigma an = C(Cl) + \mathrm{C}(\mathrm{SO_4}) + C(HCO_3)$$

Then the percentage of chloride, %Cl, and bicarbonate, %HCO_3, are evaluated according to:

$$\%\mathrm{Cl} = \frac{100C(Cl)}{\Sigma an}$$

$$\%\mathrm{HCO_3} = \frac{100C(HCO_3)}{\Sigma an}$$

This plot indicates the compositional ranges for the different kinds of waters typically found in geothermal areas, such as:

1. Mature NaCl waters of neutral pH, which are rich in Cl and plot near the Cl vertex;
2. Na-HCO_3 waters here are indicated as peripheral waters;
3. Volcanic and steam heated waters, generated through absorption into groundwater of either high-temperature HCl-bearing volcanic gases or lower-temperature H_2S-bearing geothermal vapours.

3.3 The Na-K-Mg triangular plot

The Na-K-Mg triangular plot is a method used to assess the degree of attainment of water-rock equilibrium. In this Na-K-Mg plot, the two systems are presented by two sets of lines of constant Na/K ratios and K/√Mg, radiating from the √Mg vertex and the Na vertex, respectively. Since each value of the Na/K ratio and K/√Mg ratio corresponds to a unique temperature value, each of these lines is an isotherm. The intersections of the Na-K and K-Mg isotherms, referring to the same temperatures, correspond to water compositions in equilibrium with the mineral phases controlling both geothermometers and delineate the so-called "full-equilibrium" curve. The compositions of water generated through biochemical dissolution of average crustal rocks, also shown in this triangular plot, delineate a rock dissolution area, which is well distinct from the "full-equilibrium" curve.

Samples from deep geothermal wells generally plot on the full equilibrium curve, at temperatures slightly higher than those physically measured in these wells. Corresponding spring waters plot below the full equilibrium curve and are shifted towards the $Mg^{1/2}$ vertex, indicating that, upon cooling, Mg acquisition by thermal waters proceeds faster than Na acquisition.

Some bicarbonate waters indicate attainment of partial equilibrium, whereas other CO_2-rich waters and acid waters are situated close to the $Mg^{1/2}$ vertex. These are the so called "immature waters", which provide unreliable Na-K temperatures, whereas their K-Mg temperatures may still be valid, at least for not too acidic waters.

3.4 Mineral saturation

Evaluation of chemical equilibria between minerals and aqueous solutions in natural systems requires the determination of the activities of aqueous species and knowledge of the solubilities of the minerals present in the bedrock. An assumption of specific mineral-solution equilibria is necessary to use in applying geochemistry to obtain an understanding of various physical features of a geothermal system. In this study, the WATCH chemical speciation program version 2.1A (Bjarnason, 1994) was used to calculate aquifer water compositions from the analytical data for some water and steam samples collected at the wellheads. The saturation index of several minerals is computed as a function of temperature and if the saturation indices of the minerals converge to zero (saturation) at a specific temperature, that temperature is taken to represent the reservoir temperature.

However, it is to be noted that care should be taken in interpreting the results of multi-mineral/solute equilibria, as the results depend on both the thermodynamic data base used for mineral solubilities and the activities of end-member minerals in solid solutions (Tole et al., 1993). Using the results of the aqueous speciation calculations, the saturation indices (SI) of minerals in aqueous solutions at different temperatures were computed as:

$$SI = \log Q - \log K = \log (Q/K)$$

where Q is the calculated ion activity product (IAP); and
K is the equilibrium constant.

The *SI* value for each mineral is a measure of the saturation state of the water phase with respect to the mineral phase. Values of *SI* greater than, equal to, and less than zero represent super saturation, equilibrium and under saturation, respectively, for the mineral phase with respect to the aqueous solution. Equilibrium constants for mineral dissolution often vary strongly with temperature. Therefore, if the *SI,* with respect to several minerals, converges to zero at a particular temperature, that temperature is taken to be the reservoir temperature. For the WATCH calculations of aquifer water compositions, it was assumed that the cause of the excess enthalpy was phase segregation in the producing aquifer (Arnórsson, 2000; Gudmundsson and Arnórsson, 2005).

4. HVERAVELLIR HIGH-TEMPERATURE FIELD, ICELAND

4.1 Geology

The geological units of the area from the oldest to the youngest units are as follows (Figure 3):

- Rhyolite
- Interglacial lavas and hyaloclastite
- Moraines and glaciofluvial sediments
- Recent lava

Exposures on the glacial outwash plains indicate that the rocks in the vicinity of the thermal field are hyaloclastites.

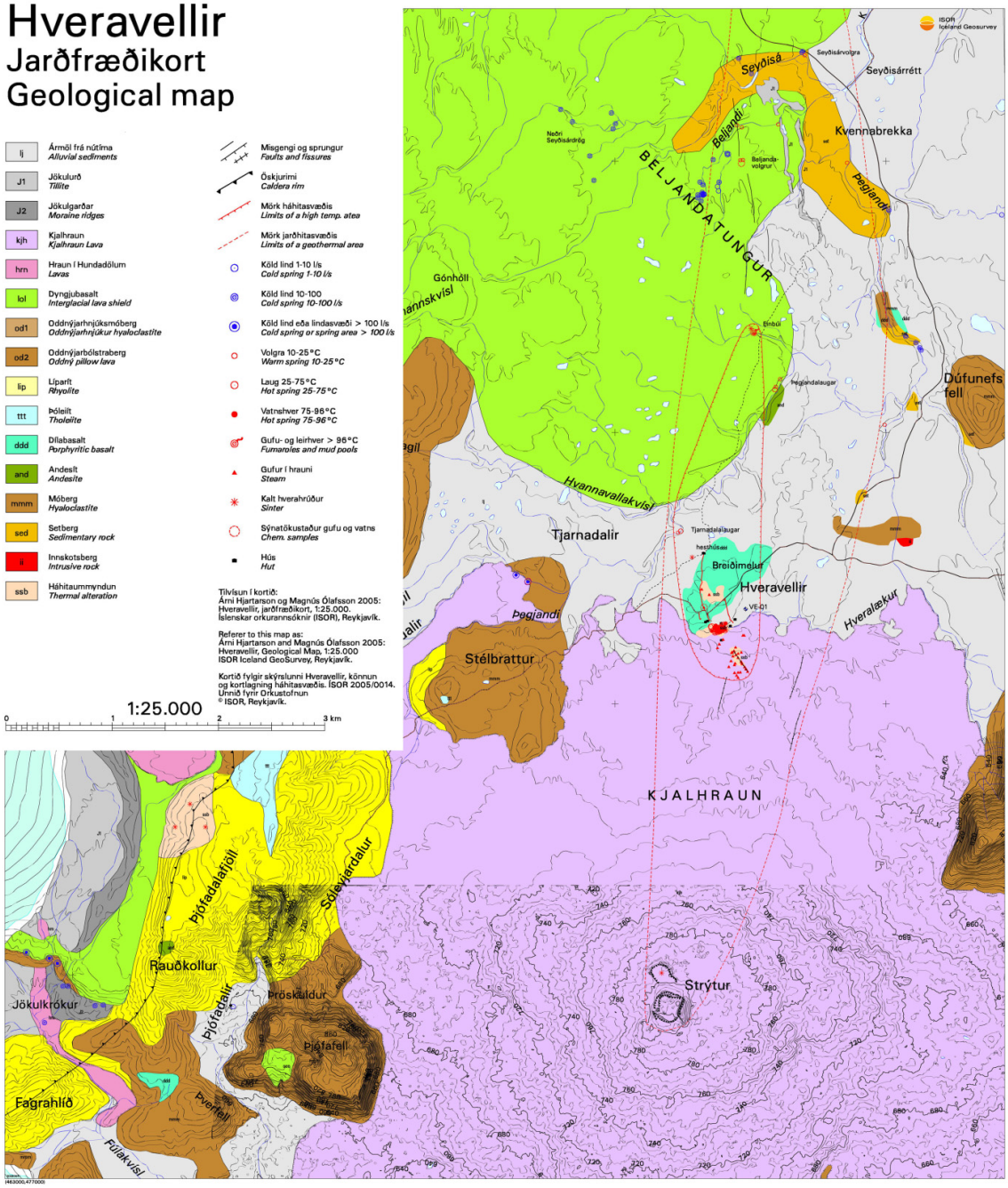

FIGURE 3: Geological map of Hveravellir

Hveravellir is one of Iceland's high-temperature fields located in central Iceland at an elevation of 630 m between the icecaps of Hofsjökull and Langjökull. The main hot springs emerge in an glacial outwash plain by the northern edge of the post glacial lava field of Kjalhraun (a lava shield), but fumarolic activity occurs in the lava field. Exposures on the glacial outwash plains indicate that the rocks in the vicinity of the thermal field are basaltic hyaloclastites and interglacial lavas. Rhyolitic rocks outcrop in several localities in the marginal mountains of Langjökull some 5 km to the west. This geothermal field is very small. The main area of alkaline hot springs is only about 0.5-1 km to the south in the Kjalhraun lava field and hydrothermal clay formed by acid surface leaching has been found several hundreds of metres northwest of the main hot springs. The area of the high-temperature field is 2.5 km^2 according to surface manifestations. The total quantity of water discharged from the hot springs has been estimated to be some 15 l/s.

4.2 Hydrogeology

The Hveravellir high-temperature field is inside the catchment area of Seydisa River (330 km^2) that is a tributary of the large glacial river Blanda with a total catchment area of 2370 km^2. Seydisá is a spring fed river with individual springs and spring areas issuing hundreds of litres per second, totalling 6 m^3/s and covering an area of 330 km^2 respectively. The aquifer is an extensive interglacial lava and underlying hyaloclastite formations. The groundwater temperature is between 2.5 and 4.5°C in most springs.

The thermal activity at Hveravellir bears close resemblance to that in the Geyser field, that is, alkaline spring waters, geysers, extensive silica sinter deposits, some mud pools, fumaroles and clayey hydrothermal soil (Figures 4 and 5). The surface manifestations are spread on a north-south line, coinciding with the active tectonic fracturing of the region (Hjartarson and Ólafsson, 2005).

FIGURE 4: An extinct geyser at Hveravellir

FIGURE 5: An active hot spring at Hveravellir

4.3 Chemical composition of the Hveravellir water samples

The geothermal samples of Hveravellir were collected from fumaroles, hot springs, warm springs and cold springs. Chemical analysis for Ca^{+2}, Na^{+}, K^{+}, Mg^{++}, SiO_2-, CO_2, SO_4, F, B and total dissolved solids (TDS) were carried out. Analysis of the water samples from Hveravellir are shown in Table 3.

4.3.1 Binary plots

Chloride has a mobile behaviour in most natural waters. Saturation with respect to halite, which determines a compatible behaviour of chloride, can be confidently used as the mobile species of reference to investigate the behaviour of other dissolved constituents. Such an investigation is

TABLE 3: Chemical composition of Hveravellir water samples, in ppm
(from Hjartarson and Ólafsson, 2005)

Sample no.	pH	Co_2	H_2S	SiO_2	B	Na	K	Mg	Ca	F	Cl	SO_4	P	Al	Fe	TDS
20040317	9.77/19.5	12.6	3.12	648	0.5	162	14.8	0.008	2.33	3.23	64.5	148	0.00315	0.126	0.0031	1000
20040318	8.64/20.1	73.7	1.02	549	0.5	162	14.2	0.01	2.53	3.13	63	154	0.003	0.05	0.0017	950
20040319	9.35/20.9	38.2	3.12	437	0.5	142	7.15	0.01	3.75	2.42	55	143	0.0032	0.07	0	790
20040320	9.60/21.8	32.8	3.34	662	0.5	163	15.6	0.01	2.67	3.3	66	152	<0.001	0.12	0.0004	1000
20040321	9.67/222.7	22.3	3.45	654	0.6	165	15.5	0.01	2.68	3.3	65	150	0.0015	0.11	<0.0004	1000
20040322	8.80/23.3	43.2	0.19	241	0.4	122	4.82	0.05	5.76	1.71	52	135	0.0088	0.05	0.0039	577
20040325	9.49/22.3	23.5	2.02	42.5	0.7	142	10.6	0.02	4.14	2.25	65	134	0.0023	0.19	<0.0004	840
20040326	7.89/22.6	45.3	<0.03	42.5	0.1	20.8	2.05	1.54	6.69	0.23	8	10.4	0.0551	0.01	<0.0004	103
20040323	7.16/22.5	27.5	<0.03	14.5	0	4.46	0.28	1.43	6.51	0.05	2.2	1.73	0.0183	0	<0.0004	34

conveniently carried out by means of binary diagrams. As a result, in this study, binary plots of Cl vs. B and TDS and Cl vs. cations were plotted (Figure 6). The TDS values ranging from 34 to 1000 ppm are directly proportional to Cl. Mg concentration is slightly higher with increasing Cl concentrations, indicative of mixing of cold water, but boron concentration increases with increasing Cl concentrations, showing a linear pattern.

4.3.2 Ternary diagrams

The Cl-SO_4-HCO_3 diagram. Seven out of the nine samples from Hveravellir lie inside the mature water field of the diagram showing mineral equilibrium (Figure 7). One sample, which is the sample from a warm spring, lies on the boundary between mature water and steam heated water, which shows mixing of geothermal water and cold water. The origin of the geothermal water can be either from direct precipitation from colder periods in the past centuries or recharge from the two big glaciers, Langjökull and/or Hofsjökull. The rest samples are situated in the area of steam heated waters.

Na-K-Mg ternary diagram. The Na-K-Mg plot for Hveravellir water samples (Figure 8) shows that the $T_{K\text{-}Na}$ values range between 140 and 220°C which is in a good agreement with the calculated Na-K temperatures. Two samples show higher magnesium concentrations, probably a result of mixing with cold groundwater.

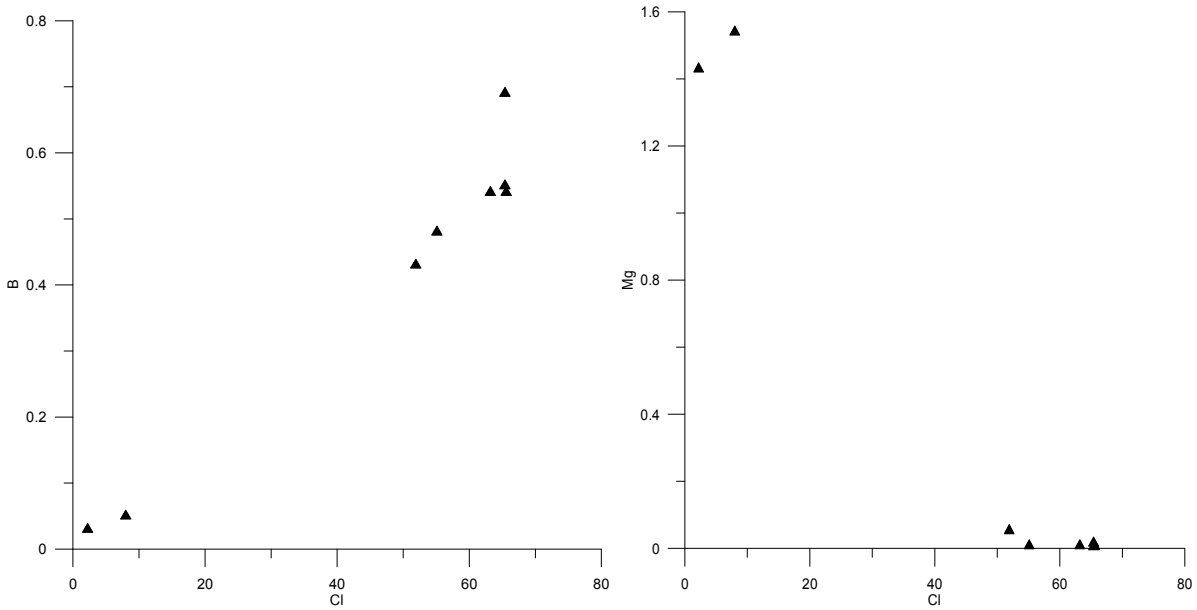

FIGURE 6: Binary plots of Cl vs. cations, B, TDS
for Hveravellir water samples, units are in ppm

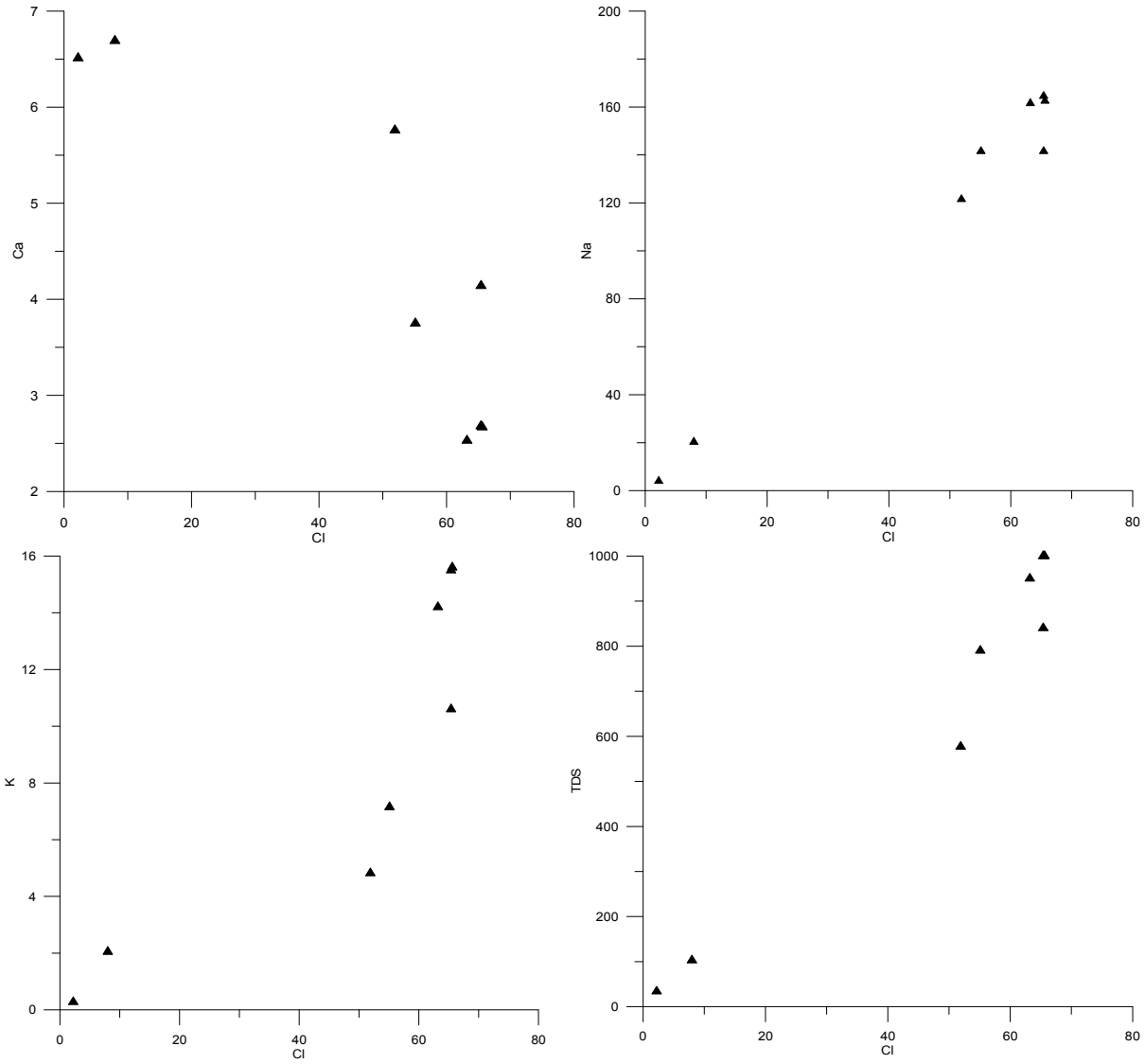

FIGURE 6 cont.: Binary plots of Cl vs. cations, B, TDS for Hveravellir water samples, units are in ppm

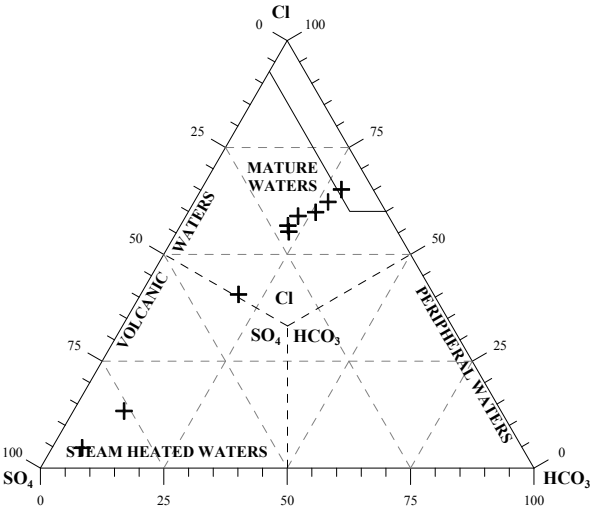

FIGURE 7: Cl-SO_4-HCO_3 plot for Hveravellir water samples

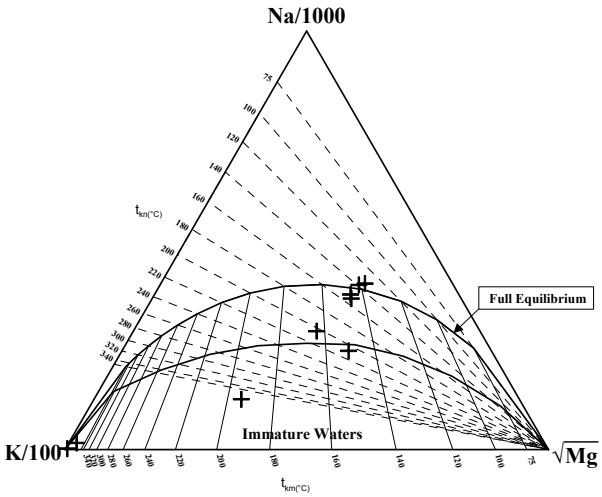

FIGURE 8: Na-K-Mg ternary plot for Hveravellir water samples

4.3.3 Geothermometry of Hveravellir water

In this study, various silica and Na-K geothermometers were applied to evaluate the reservoir temperature of Hveravellir geothermal field. The results are listed in Tables 4 and 5. The average temperature for the area, derived from the different temperature equations for the silica geothermometer that were applied in this study, was found to be 238°C. The temperature values of Fournier and Potter (1982) and Arnórsson (2000) in Equation 4 are higher than that of Fournier (1977) in Equation 2.

The average temperature value of the area, based on equations for the Na-K geothermometers, is 183°C which differs some with the calculated value of the silica geothermometer but seems to agree with the value from the Na-K-Mg ternary plot which gave temperature values between 140 and 220°C.

TABLE 4: Results of silica geothermometers for Hveravellir water samples (°C)

Sample no.	F1	F2	FP	A	Average
20040317	277	244	361	391	318
20040318	261	232	327	349	292
20040319	240	216	287	301	261
20040320	279	246	366	397	322
20040321	278	245	363	393	320
20040322	193	178	211	210	198
20040325	260	231	325	347	291
20040326	94	96	95	81	92
20040323	51	58	51	36	49

F1, F2: Fournier (1977), Equations 1 and 2, respectively;
FP: Fournier and Potter (1982); A: Arnórsson (2000) Equation 4.

TABLE 5: Results of Na-K geothermometers for Hveravellir water samples (°C)

Sample no.	TM	Tr	F	To	A1	FT	Gig	A2	Average
20040317	96.4	178	218	185	186	196	225	209	200
20040318	93.5	174	215	180	182	193	222	205	196
20040319	97.6	124	172	128	134	152	183	167	151
20040320	96.5	183	222	190	191	200	229	212	204
20040321	99.1	181	221	188	189	199	227	211	202
20040322	97.3	105	155	108	116	137	168	152	134
20040325	98.0	158	201	164	167	180	210	194	182
20040326	20.3	186	225	193	194	203	231	214	206
20040323	1.8	142	188	147	152	168	198	181	168

TM: Measured temperature; A1 and A2: Arnórsson et al. (1983) Equations 13 and 14;
Tr: Truesdell (1976); F: Fournier (1979); FT: Na-K-Ca geothermometer;
Gig: Giggenbach et al. (1983); (Fournier and Truesdell, 1973); To: Tonani (1980).

5. THE TENDAHO HIGH-TEMPERATURE GEOTHERMAL FIELD

5.1 Geology of Tendaho

The Tendaho geothermal field is located in the Afar depression, a plate tectonic triple junction where the spreading ridges that are forming the Red Sea and the Gulf of Aden emerge on land and meet the East African rift. The Tendaho geothermal field in Afar consists of a NW-SE elongated broad plain of about 4000 km^2 (Tendaho Graben – Figure 9) mainly filled by alluvial and lacustrine deposits (Aquater, 1996). The oldest volcanic products in the area are lava pile outcroppings on the graben

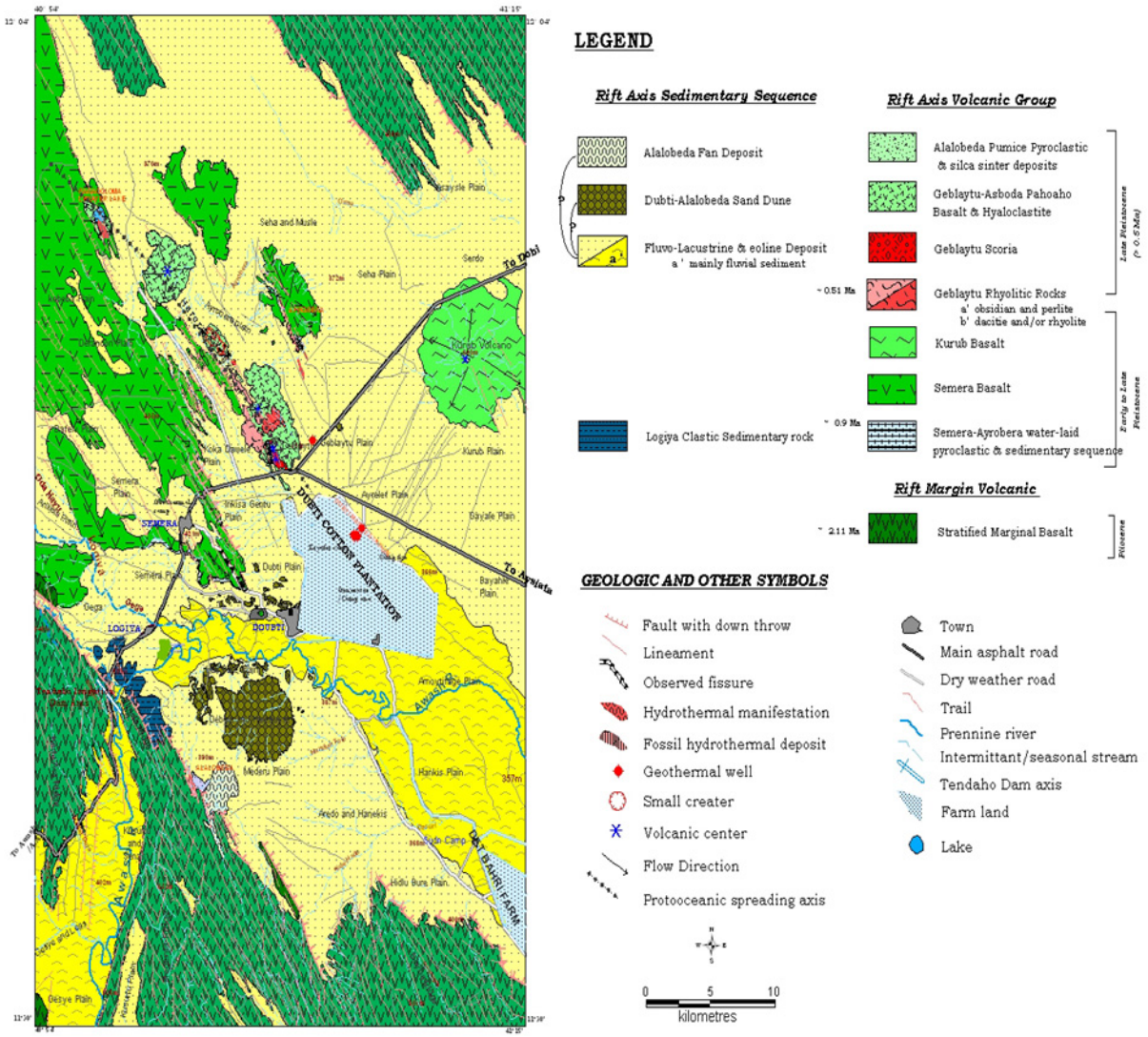

FIGURE 9: Geological map of the Tendaho area (Megersa and Getaneh, 2006)

edges (Afar stratoid series), whereas the most recent activity, both linear and central, is concentrated within the graben.

Recent volcanoes in the graben from northwest to southeast include: The Manda Hararo complex, Kurub volcano, Dama Ali and Gabilima volcanoes. The nature of the volcanoes is discussed below, mainly based on Sibert and Simkin (2005). The Manda Hararo complex is the southernmost axial range of western Afar with a summit elevation of about 600 m. The massive complex is 105 km long and 20-30 km wide, and represents an uplifted segment of a mid-oceanic ridge spreading centre. The dominant part of the complex lies to the south. Hot springs and fumaroles occur around Begaloma Crater Lake. Extensive hydrothermal manifestations occur at Ayrobera on the southeastern tip of the complex (Kebede, 2005).

Kurub shield volcano lies in the Saha plain, southeast of the Manda Hararo complex. Its summit elevation is 625 m a.s.l. Windblown sand fills the summit crater of the volcano. Initial subaqueous activity occurred along north-northwest trending fissures.

Dama Ali is a broad shield volcano that rises above the northwest shore of Lake Abhe, southwest of Tendaho. Its summit elevation is 1068 m a.s.l. The 25 km wide volcano has an arcuate chain of rhyolitic lava domes occupying the northern, western and southern flanks. Dama Ali is considered the

most likely source of an eruption that was reported to have occurred in 1631. Major fumarolic activity occurs in the summit crater and abundant hot springs are found on the volcano.

Galima is a strato volcano with a summit elevation of 1459 m a.s.l. and is located at the intersection of the central Afar rift zone with the northern end of the NE-SW trending main Ethiopian rift. Rhyolitic lava domes are located on the flanks of the volcano and a 5×17 km basaltic lava field covers the plain north of the volcano.

The most recent stage of volcanism is associated with remnant magmatic bodies that are partially destined to cool at varying depths under the rift floor. Waters of meteoric origin migrate to these depths, heat up and re-emerge on the surface to form the various hydrothermal manifestations.

5.2 Hydrogeology and geothermal activity of Tendaho

The major river draining the Tendaho Graben is Awash River (Figure 9). The river starts in the highland of central Ethiopia, at an altitude of about 3000 m a.s.l. and after flowing southeast for about 250 km, enters the Rift Valley and then follows the valley for the rest of its course to Lake Abe on the border with the Djibouti Republic. The Awash River basin is divided into 3 sub-catchments: upper (upstream from Koka Dam station), middle (between Koka and Awash station), and lower (between Awash and Tendaho station) (Hailemariam, 1999). The river passes about 10 km south of the area where geothermal drilling has taken place and is characterised by extensive variations of flow throughout the year, the maximum being from September to October. Groundwater aquifers of the region include coarse sedimentary and fractured volcanic units. Subsurface stratigraphy in the drilled area shows that the Tendaho Graben is filled with: an upper thick sedimentary sequence consisting of fine- to medium-grained sandstone, siltstone and clay, intercalated by basaltic lava sheets; and lower basaltic lava flows of the Afar Stratoid series. The upper sequence has permeable zones at intervals, while poor permeability is indicated in the drilled Afar stratoid series.

Hydrothermal manifestations, both active and extinct, can be observed in the Tendaho graben (Figure 10). The active manifestations occur in various parts of the graben. High-temperature fumaroles and an associated extensively altered area occur at Arobeyra, aligned along a NW-SE trending structure. Several mud pots and fumaroles emerge from sediments near Doubti geothermal wells. Erupting hot springs (near or at boiling point), silica sinter depositions and fumaroles occur at Alalobeda, about 6 km southwest of the initial development area. An extinct hydrothermal system indicated by silica deposition occurs southeast of Logia within an area where northwest to north-northwest trending sub vertical fractures cross cut the rift sediment.

FIGURE 10: Boiling hot spring at Tendaho

5.3 Chemical composition of Tendaho geothermal fluids

The geothermal water samples of Tendaho were collected from well TD-6, a test well (Ali and Gizawe, 2000). Chemical analyses for Na, K, Ca, Mg, CO_3, HCO_3, Cl, SO_4, F, NO_3, OH, B, and SiO_2 were carried out. Analysis of the water samples from Tendaho are shown in Table 6.

TABLE 6: Chemical compositions of Tendaho water samples, in ppm (Ali, 2000)

Location	Sample no.	pH	cond.	Na	K	Ca	Mg	CO_3	Cl	SO_4	F	NO_3	OH	B	SiO_2	HCO_3
TD-6	1	9.5	3171	635	77	10	2	108	1000	156	1.57	1.68	9	4	544	94.07
"	2	9.51	3019	600	68	10	1	101	890	136	1.65	0.82	9	4.1	526	88.37
"	3	9.53	3052	585	68	9	0.1	82	886	124	1.56	0.79	13	4.3	500	72.68
"	4	9.58	3074	590	68	13	0.1	86	896	149	1.44	1.37	8	4.2	530	74.31
"	5	9.49	3054	600	69	10	0.01	82	890	122	1.42	1.34	10	4.1	493	71.88
"	6	9.49	3049	585	68	10	0.01	86	890	132	1.4	1.42	7	4.1	489	75.69
"	7	9.49	3061	585	68	10	0.01	77	865	130	1.43	1.39	8	4.3	489	67.52
"	8	9.45	3052	585	68	11	0.01	77	865	134	1.38	1.6	8	4.4	598	62.6
"	9	9.42	3016	565	66	12	0.01	79	890	134	1.4	1.54	8	4.3	478	67.84
Allalobeda	10	9.01	2973	580	36	29	0.01	20	805	306	0.76	1.12		1.9	348	15.53
TD-6	11	9.45	3035	610	70	12	0.01	84	886	279	1.38	1.49	5	4	489	73.41
"	12	9.52	2955	570	73	9	0.3	108	833	157	1.34	0.5	9	3.7	578	93.32
"	13	9.46	3121	560	67	11	0.01	84	869	144	1.4	1.39	10	4.1	500	72.61

5.3.1 Binary plots

Binary plots of Cl vs. cations, B and SiO_2 were plotted (Figure 11). The concentration of Mg is lower with increasing Cl concentration which indicates mixing of cold groundwater with the geothermal water. Boron concentration is almost unchanged with increasing Cl concentration.

5.3.2 Ternary diagrams

Cl-SO_4-HCO_3 diagram: All the samples taken from well TD-6 of Tendaho geothermal field lie in the area for "mature waters" indicating that the water type is deep NaCl, rich in Cl, neutral pH and there is equilibrium between the rock and the minerals (Figure 12).

The Na-K-Mg diagram for the Tendaho well samples (Figures 13) shows that the $T_{K\text{-}Na}$ values range between 160 and 220°C which is in good agreement with the calculated values of both silica and Na-K temperatures. Two samples fall in the area of "immature waters" indicating that there was a mixing between geothermal water and cold sea water in ancient times.

5.3.3 Geothermometry of the Tendaho water

The results of the silica and Na-K geothermometers are listed in Tables 7 and 8, respectively. The

TABLE 7: Results of silica geothermometers for Tendaho water (°C)

Sample no.	F2	F1	FP3	A1	A2	Average	F3	A4
TD6-1	232	260	268	278	286	265	255	238
TD6-2	229	257	264	272	274	259	251	235
TD6-3	226	252	258	264	259	252	245	230
TD6-4	230	257	265	274	277	260	252	236
TD6-5	225	251	256	262	255	250	244	228
TD6-6	224	250	255	261	253	249	243	228
TD6-7	224	250	255	261	253	249	243	228
TD6-8	239	269	281	297	322	281	266	248
TD6-9	223	248	253	258	247	246	240	225
TD6-10	201	221	223	221	187	211	207	196
TD6-11	224	250	255.	261	253	249	243	228
TD6-12	236	266	276	290	308	275	262	245
TD6-13	225	252	258	264	259	252	245	230

F1 and F2 – Fournier (1977) Equations 1 and 2, respectively; F3 – Fournier (1977) Equation 7;
FP3 – Fournier and Potter (1982); F4 – Chalcedony (Arnórsson et al., 1983);
A1 and A2 – Arnórsson (2000) Equations 4 and 5, respectively.

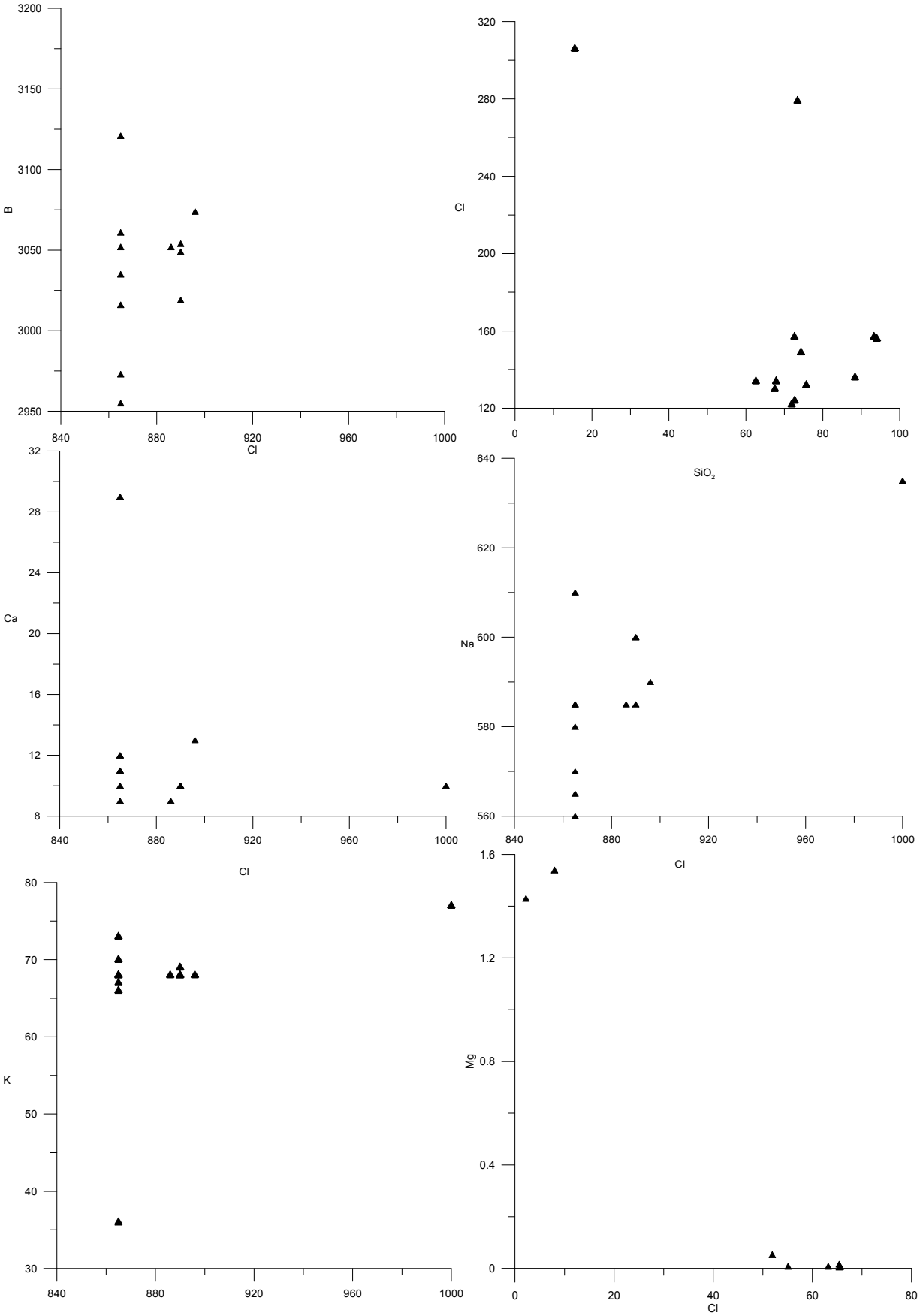

FIGURE 11: Binary plots of Cl vs. cations, B and SiO_2 for Tendaho water samples, units are in ppm

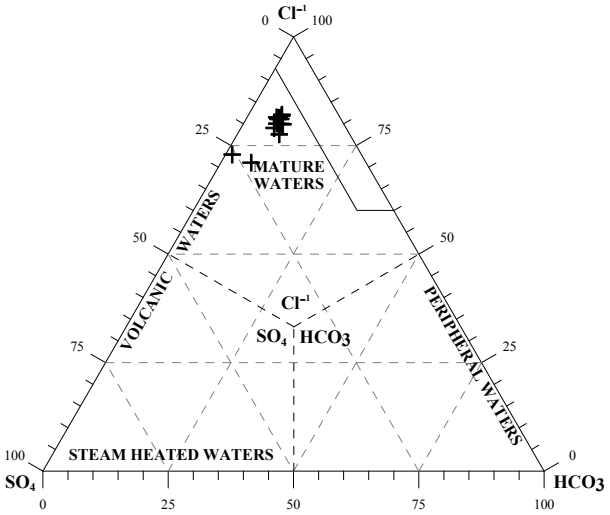

FIGURE 12: Cl-SO_4-HCO_3 plot for Tendaho water samples

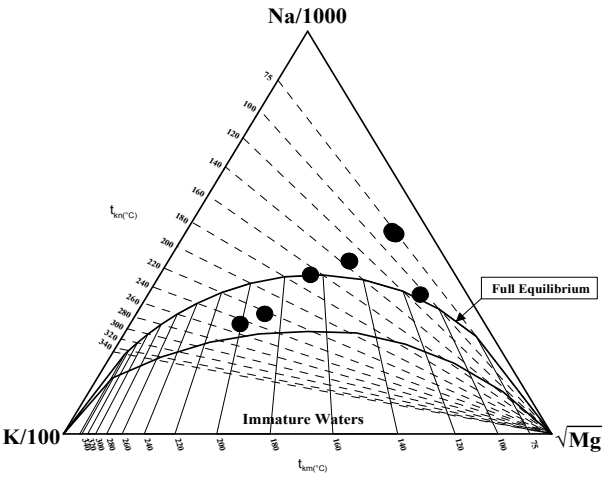

FIGURE 13: Na-K-Mg ternary plot for Tendaho water samples

results of the two types of geothermometers applied for the Tendaho water samples, the silica and Na-K geothermometers, only show slight differences. The temperature values of the silica geothermometer range between 210 and 280°C and those of the Na-K geothermometer range between 167 and 225°C.

TABLE 8: Results of the selected Na-K geothermometers for Tendaho water (°C)

Sample no.	Tr	F	To	A	Nie	FT	A	Average
TD6-1	209	243	217	215	220	247	230	226
TD6-2	203	239	211	210	216	244	227	221
TD6-3	206	241	214	212	218	246	229	223
TD6-4	203	239	211	210	216	244	227	221
TD6-5	203	239	211	210	216	244	227	221
TD6-6	206	241	214	212	218	246	229	223
TD6-7	206	241	214	212	218	246	229	223
TD6-8	206	241	214	212	218	246	229	223
TD6-9	206	241	214	212	218	246	229	223
TD6-10	141	186	145	150	166	196	180	167
TD6-11	203	239	211	210	216	244	227	221
TD6-12	217	250	226	222	226	253	236	233
TD6-13	209	243	217	215	220	247	230	226

Tr – Truesdell (1976); Nie – Nieva and Nieva (1987); F – Fournier (1979);
FT – Na-K-Ca geothermometer (Fournier and Truesdell, 1973); To – Tonani (1980);
A1 and A2 – Arnórsson et al. (1983) Equations 13 and 14.

6. COMPARISON

The results of the geochemical methods in this study can be used to compare the two high-temperature fields, Hveravellir, Central Iceland and Tendaho in N-Ethiopia.

Similarities:

- Water type – both NaCl type.
- Reservoir temperature:
  - — Hveravellir 160-220°C;
  - — Tendaho 140-220°C.

- High silica content:
  - Hveravellir – reaches up to 662 mg/l;
  - Tendaho – reaches up to 598 mg/l.
- Both show cold water mixing in the upflow zone.

Dissimilarities:

- Origin of cold water mixing:
  - Hveravellir – cold water precipitation during ancient time or recharge from neighbouring glaciers;
  - Tendaho – sea water during ancient time.

7. CONCLUSIONS

Various geochemical methods were applied in this study. These methods help predict the reservoir temperature and processes (such as mixing and boiling) affecting the equilibrium condition between the mineral and rocks in the upflow zone of the reservoir.

The geothermal springs at Hveravellir are higher in silica than most of the geothermal springs in Iceland, the highest being 662 mg/l, that may be due to the rising water level of the area. The water has boiled and mixed with cold water in the upflow zone. Na-K-Mg triangular plot gave a temperature value of 140-220°C. The silica geothermometers, applicable for high-temperature fields, gave a value ranging between 197 and 319°C. The wide range of the values may be the result of mixing.

The silica geothermometer result for the Tendaho geothermal field is between 210 and 280°C. This value are in disagreement with the Na-K-Mg triangular plot but some agreement with the Na-K geothermometer which gave values ranging between 167 and 225°C. Again, this shows mixing of cold water with the geothermal water.

ACKNOWLEDGEMENTS

I would like to thank all the staff of UNU-GTP for their endless support during our training. My special thanks go to Dr. Ingvar Birgir Fridleifsson and Mr. Lúdvík S. Georgsson for their priceless contribution by giving trainees from my country a chance to help develop their potential in geothermal sciences. I also thank my supervisors, Dr. Árni Hjartarson and Ms. Kristin Kröyer, for their valuable support in preparing my project paper.

Last, but not least, my heartfelt gratitude goes to all the Orkustofnun staff who gave us all we needed in our stay and for the very welcoming and peaceful people of Iceland.

REFERENCES

Ali, S., and Gizawe, T., 2000: *Geochemical investigation of Tendaho and Allalobeda*. Geological Survey of Ethiopia, unpublished internal report.

Aquater 1996: *Tendaho geothermal project, final report.* MME – EIGS, Ehtiopia & Government of Italy, Ministry of Foreign Affairs, San Lorenzo in Campo.

Árnason, B., 1976: *Groundwater systems in Iceland traced by deuterium*. Soc. Sci. Islandica, 42, Reykjavík, 236 pp.

Arnórsson, S. (ed.), 2000: *Isotopic and chemical techniques in geothermal exploration, development and use. Sampling methods, data handling and interpretation*. International Atomic Energy Agency, Vienna, 351 pp.

Arnórsson, S., Gunnlaugsson, E., and Svavarsson, H., 1983: *The chemistry of geothermal waters in Iceland. III. Chemical geothermometry in geothermal investigations*. *Geochim. Cosmochim. Acta, 47*, 567-577.

Bjarnason, J.Ö., 1994: *The speciation program WATCH, version 2.1.* Orkustofnun, Reykjavík, 7 pp.

Björnsson, A., 1985: Dynamics of crustal rifting in north-eastern Iceland. *J. Geophys. Res., 90-B12,* 10.151-10.162.

D'Amore, F., and Arnórsson, S., 2000: Geothermometry. In: Arnórsson, S. (ed.), *Isotopic and chemical techniques in geothermal exploration, development and use. Sampling methods, data handling, interpretation*. International Atomic Energy Agency, Vienna, 152-199.

Ellis, A.J., and Mahon, W.A.J., 1977: *Chemistry and geothermal systems.* Academic Press, New York, 392 pp.

Ellis, A.J., and Wilson, S.H., 1960: The geochemistry of alkali metals ions in the Wairakei hydrothermal system, *N.Z.J. Geol. Geophys., 3*, 593-617.

Fahlquist, L., and Janik, C.J., 1992: *Procedures for collecting and analysing gas samples from geothermal systems*. US Geological Survey, report 92-211, 19 pp.

Fournier, R.O., 1977: Chemical geothermometers and mixing model for geothermal systems. *Geothermics, 5,* 41-50.

Fournier, R.O., 1979: A revised equation for Na-K geothermometer. *Geoth. Res. Council, Trans., 3,* 221-224.

Fournier, R.O., 1981: Application of water chemistry to geothermal exploration and reservoir engineering. In: Rybach, L., and Muffler, L.J.P. (editors), *Geothermal system: Principles and case histories.* John Wiley and Sons Ltd., Chichester, 109-143.

Fournier, R.O., and Potter, R.W., 1982: An equation correlating the solubility of quartz in water from 25° to 900°C at pressures up to 10,000 bars. *Geochim. Cosmochim. Acta, 46*, 1969-1973.

Fournier, R.O., and Rowe, J.J., 1962: The solubility of cristobalite along the three-phase curve, gas plus liquid plus cristobalite. *Am. Mineralogist, 47*, 897-902.

Fournier, R.O., and Truesdell, A.H., 1973: An empirical Na-K-Ca geothermometer for natural waters. *Geochim. Cosmochim. Acta*, *37*, 1255-1275.

Giggenbach, W.F., 1988: Geothermal solute equilibria. Derivation of Na-K-Mg-Ca geoindicators. *Geochim. Cosmochim. Acta, 52*, 2749-2765.

Giggenbach, W.F., and Goguel, R.L., 1989: *Collection and analysis of geothermal and volcanic water and gas discharges*. Department of Scientific and Industrial Research, New Zealand, report CD2401, 81 pp.

Giggenbach, W.F., Gonfiantini, R., Jangi, B.L., and Truesdell, A.H., 1983: Isotopic and chemical composition of Parbati Valley geothermal discharges, NW Himalaya, India. *Geothermics, 12*, 199-222.

Gudmundsson, B.T., and Arnórsson, S., 2005: Secondary mineral-fluid equilibria in the Krafla and Námafjall geothermal systems, Iceland. *Applied Geochemistry, 20,* 1607-1625.

Hailemariam, K., 1999: Impact of climate change on the water resources of Awash river basin, Ethiopia. *Climate Research, 12,* 6 pp.

Hjartarson, A., and Ólafsson, M., 2005: *Hveravellir, Geological map, 1:25,000.* ISOR- Iceland Geosurvey, Reykjavik.

Kebede, S., 2005: Preliminary environmental impact assessment for the development of the Tendaho geothermal area, Ethiopia. Report 11 in: *Geothermal Training in Iceland 2005.* UNU-GTP, Iceland, 137-162.

Megersa, G., and Getaneh, E., 2006: *Geological, surface hydrothermal alteration and geothermal mapping of Dubti-Semera area, Tendaho geothermal field.* GSE, Addis Ababa, unpubl. report, 66 pp.

Morey, G.W., Fournier, R.O., and Rowe, J.J., 1962: The solubility of quartz in water in the temperature interval from 29 to 300°C. *Geochim. Cosmochim. Acta, 26,* 1029-1043.

Nieva, D., and Nieva, R., 1987: Developments in geothermal energy in Mexico, part 12-A cationic composition geothermometer for prospection of geothermal resources. *Heat Recovery and CHP, 7,* 541-544.

Orville, P.M., 1963: Alcali ion exchange between vapour and feldspar phases. *Am. J. Sci., 261*, 201-237.

Siebert, L., and Simkin, T., 2005: *Volcanoes of the world: an illustrated catalogue of Holocene volcanoes and their eruptions.* Smithsonian Institution, Global Volcanism Program Digital Information Series, GVP-3, internet website: *http://www.volcano.si.edu/world/.*

Tole, M.P., Ármannsson, H., Pang Z.H., and Arnórsson, S., 1993: Fluid/mineral equilibrium calculations for geothermal fluids and chemical geothermometry. *Geothermics, 22*, 17-37.

Tonani, F., 1980: Some remarks on the application of geothermal techniques in geothermal exploration. *Proceedings of 2nd Symposium of Advanced European Geothermal Research., Strassbourg,* 428-443.

Truesdell, A.H., 1976: Summary of section III - geochemical techniques in exploration. *Proceedings of 2nd U.N. Symposium on the Development and Use of Geothermal Resources, San Francisco, 1,* liii-lxxix.

Truesdell, A.H., and Fournier, R.O., 1976: Calculations of deep temperatures in geothermal systems from the chemistry of boiling spring waters of mixed origin. *Proceedings of 2nd U.N. Symposium on the Development and Use of Geothermal Resources, San Francisco, 1,* 837-844.

Truesdell, A.H., and Hulston, J.R., 1980: Isotopic evidence of environments of geothermal systems, In: Fritz, P., and Fontes, J.C., (editors), *Handbook of Environmental Isotope Chemistry.* Elsevier, New York, 179-226.

UNDP, 1973: *Geology, geochemistry and hydrology of hot springs of the East African Rift System within Ethiopia*. UNDP, December report DD/SF/ON/11, NY.

White, D.E., 1965: Saline waters of sedimentary rocks. *Am. Assoc. Petrol. Geol., Mem. 4,* 352-366.